VOLUME 70, NUMBER 22

JOC Articles

OCTOBER 28, 2005

Ab Initio Molecular Orbital and Density Functional Studies on the Solvolysis of Sarin and *O*,*S*-Dimethyl Methylphosphonothiolate, a VX-like Compound

Jolita Šečkutė,[†,1] Jessica L. Menke,[†] Ryan J. Emnett,[†,2] Eric V. Patterson,[†,*] and Christopher J. Cramer[‡]

Truman State University, Division of Science, 100 East Normal Street, Kirksville, Missouri 63501-4221, and Department of Chemistry and Supercomputer Institute, University of Minnesota, 207 Pleasant Street SE, Minneapolis, Minnesota 55455-0431

epatters@truman.edu

Received February 10, 2005

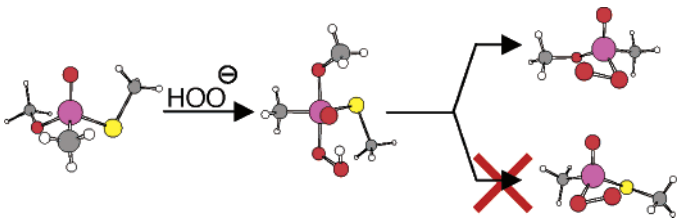

Potential energy surfaces for the alkaline hydrolysis of sarin and *O*,*S*-dimethyl methylphosphonothiolate, a VX model compound, and the perhydrolysis of the latter have been computed at the MP2/6-31+G(d)//mPW1K/MIDI! level of theory. The effect of aqueous solvation was accounted for via the integral equation formalism polarizable continuum model (IEF-PCM) at the HF/6-31+G(d) level. Excellent agreement with the experimental enthalpy of activation for alkaline hydrolysis of sarin was found. For the alkaline hydrolysis of *O*,*S*-dimethyl methylphosphonothiolate, it was found that the P−O and P−S bond cleavage processes are kinetically competitive but that the products of P−S bond cleavage are thermodynamically favored. For the perhydrolysis of *O*,*S*-dimethyl methylphosphonothiolate, it was found that P−O bond cleavage is not kinetically competitive with P−S bond cleavage. In both cases, the data support initial formation of trigonal bipyramidal intermediates and demonstrate kinetic selectivity for nucleophilic attack on the face opposite the more apicophilic methoxide ligand.

Introduction

Recent years have seen a sharp increase in concern regarding the use of chemical and biological weapons as agents of terror. Such fears proved well-founded in 1995 when the Aum Shinrikyo cult launched an attack on the Tokyo subway system using a crude form of sarin (*O*-isopropyl methylphosphonofluoridate, **1a**), a potent, irreversible acetylcholinesterase inhibitor.[3] This attack killed 12 and injured over 5000.[4−7] A related compound, VX [*O*-ethyl *S*-(2-diisopropylamino)ethyl methylphosphonothiolate, **1b**], has also made headlines as fears sur-

* To whom correspondence should be addressed.
† Truman State University.
‡ University of Minnesota.

(1) Present address: Department of Chemistry and Chemical Biology, Cornell University, Ithaca, NY 14853-1301.
(2) Present address: Saint Louis University School of Medicine, St. Louis, MO 63104.
(3) Benschop, H. P.; DeJong, L. P. A. *Acc. Chem. Res.* **1988**, *21*, 368−374.
(4) Nozaki, H.; Aikawa, N. *Lancet* **1995**, *345*, 1446−1447.
(5) Suzuki, T.; Morita, H.; Ono, K.; Maekawa, K.; Nagai, R.; Yazaki, Y. *Lancet* **1995**, *345*, 980−981.
(6) Masuda, N.; Takatsu, M.; Marinari, H.; Ozawa, T. *Lancet* **1995**, *345*, 1446.
(7) Nagao, M.; Takatori, T.; Matsuda, Y.; Nakajima, M.; Iwase, H.; Iwadate, K. *Toxicol. Appl. Pharmacol.* **1997**, *144*, 198−203.

10.1021/jo0502706 CCC: $30.25
Published on Web 06/02/2005

SCHEME 1. General Scheme for Addition−Elimination Reactions of Organophosphorus Compounds

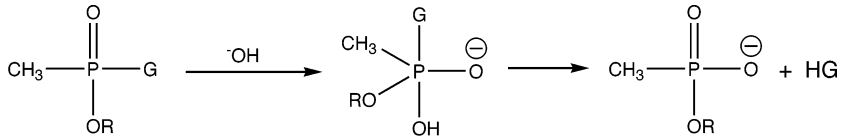

1a: G = F, R = *i*Pr (sarin) **2(a-c)** **3(a-c)**
1b: G = $SCH_2CH_2N(i\text{-}Pr)_2$, R = Et (VX)
1c: G = SCH_3, R = CH_3 (VX model)

SCHEME 2. Products from Alkaline Hydrolysis of VX and Model 1c

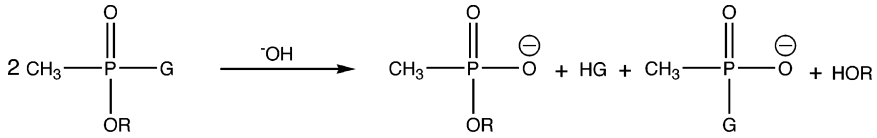

1b: G = $SCH_2CH_2N(i\text{-}Pr)_2$, R = Et (VX) **3b** (EMPA) **4b** (EA2192)
1c: G=SCH_3, R=CH_3 **3c** **4c**

rounding its use or possession by terrorist cells and rogue states have become elevated. While the biochemistries of sarin and VX are similar,[3] there are several important differences in their ex vivo chemistry.[8,9] Sarin belongs to the volatile G-series of nerve agents, while VX belongs to the nonvolatile V-series of nerve agents. Thus, VX is much more persistent than sarin, meaning that an area contaminated by VX may stay contaminated for an extended period of time, while sarin is likely to evaporate and dissipate in short order. VX is also considerably more toxic than sarin. The persistence and toxicity of VX make it imperative that as much as possible is understood concerning its neutralization chemistry.

It is well-known that G-series nerve agents such as sarin are readily neutralized by aqueous sodium hydroxide.[8,10−12] Two reports of experimental reaction barriers are found in the literature. Larsson reported an Arrhenius activation energy (E_a) of 9.1 ± 0.3 kcal/mol at pH 9 derived from rates determined between 293 and 303 K and a second-order rate constant of 25.8 M^{-1} s^{-1} at 298 K.[11] Under similar conditions, Gustafson and Martell determined the enthalpy of activation ($\Delta H^{\ddagger}$) to be 10.0 kcal/mol, with a second-order rate constant at 298 K of 25.0 M^{-1} s^{-1}.[12] Both studies observed complete hydrolysis of sarin, implying a significant negative change in free energy over the course of the reaction. The mechanism for this displacement is generally believed to be an addition−elimination pathway involving a trigonal bipyramidal intermediate (Scheme 1).[8,11,12] A recent theoretical study confirmed such a pathway and arrived at a barrier of 8.6 kcal/mol, in reasonable agreement with the experimental data.[13]

By comparison, the reaction of VX with aqueous sodium hydroxide is much slower.[8,14] The second-order rate constant for the alkaline hydrolysis of VX is 4.12 × 10^{-3} M^{-1} s^{-1} at 298 K.[15] A problematic feature of the alkaline hydrolysis of VX is that it yields a mixture of products resulting from competing P−S bond cleavage, generating ethyl methylphosphonic acid (EMPA, **3b**), and P−O bond cleavage, generating *S*-(2-diisopropylamino)-ethyl methylphosphonothioic acid (EA2192, **4b**), in a ratio of approximately 7:1 favoring EMPA (Scheme 2).[16] EA2192 (**4b**) is also a potent neurotoxin[17] and must be further hydrolyzed to effect complete detoxification. Yang et al. have determined the Arrhenius activation energies (E_a) for the competitive P−S and P−O bond cleavage steps at pH 12 to be 14.5 and 14.6 kcal/mol, respectively.[18] They also note that the activation energies drops to 12.6 and 11.1 kcal/mol, respectively, at pH 11, presumably due to intramolecular catalytic involvement of the aminothiol chain. Groenewold, Williams, and co-workers determined similar Arrhenius activation energies of 12−14 kcal/mol for the hydrolysis of VX on concrete.[19,20] Despite issues involving competing P−S and P−O bond cleavage and a slower than ideal rate, the hydrolyses of both VX and **4b** are rapid enough at elevated temperatures that the United States Army is currently pilot testing alkaline hydrolysis (pH 14, 90 °C) in conjunction with biodegradation for the bulk neutralization of stockpiled VX.[21]

The use of α-nucleophiles has been shown to be effective for the destruction of VX.[22] For example, when a solution containing the anion of hydrogen peroxide is employed, VX reacts at room temperature at a rate similar to that of sarin reacting with hydroxide, and

(8) Yang, Y.-C.; Baker, J. A.; Ward, J. R. *Chem. Rev.* **1992**, *92*, 1729−1743.
(9) Somani, M. *Chemical Warfare Agents*; Academic Press: San Diego, CA, 1992.
(10) Epstein, J.; Bauer, V. E.; Save, M.; Memek, M. M. *J. Am. Chem. Soc.* **1956**, *78*, 4068−4071.
(11) Larsson, L. *Acta Chem. Scand.* **1957**, *11*, 1131−1142.
(12) Gustafson, R. L.; Martell, A. E. *J. Am. Chem. Soc.* **1962**, *84*, 2309−2316.
(13) Zheng, F.; Zhan, C.-G.; Ornstein, R. L. *J. Chem. Soc., Perkin Trans. 2* **2001**, 2355−2363.
(14) Epstein, J.; Callahan, J. J.; Bauer, V. E. *Phosphorus* **1974**, *4*, 157−163.
(15) Yang, Y.-C.; Szafraniec, L. L.; Beaudry, W. T. *J. Org. Chem.* **1993**, *58*, 6964−6965.
(16) Yang, Y.-C. *Acc. Chem. Res.* **1999**, *32*, 109−115.
(17) Yang, Y.-C.; Szafraniec, L. L.; Beaudry, W. T.; Rohrbaugh, D. K. *J. Am. Chem. Soc.* **1990**, *112*, 6621−6627.
(18) Yang, Y.-C.; Szafraniec, L. L.; Beaudry, W. T.; Samuel, J. B.; Rohrbaugh, D. K. *Proceedings of the November 1994 ERDEC Scientific Conference of Chemical and Biological Defense Research*; Aberdeen Proving Ground, MD, 1996; pp 375−382.
(19) Groenewold, G. S.; Williams, J. M.; Appelhans, A. D.; Gresham, G. L.; Olson, J. E.; Jeffery, M. T.; Rowland, B. *Environ. Sci. Technol.* **2002**, *36*, 4790−4794.
(20) Williams, J. M.; Rowland, B.; Jeffery, M. T.; Groenewold, G. S.; Applehans, A. D.; Gresham, G. L.; Olson, J. E. *Langmuir* **2005**, *21*, 2386-2390.
(21) Irvine, R. L.; Haraburda, S. S.; Galbis-Reig, C. *Water Sci. Technol.* **2004**, *50*, 11−18.
(22) Cassagne, T.; Cristau, H.-J.; Delmas, G.; Desgranges, M.; Lion, C.; Magnaud, G.; Torreilles, E.; Virieux, D. *Heteroat. Chem.* **2001**, *12*, 485−490.

exclusive P−S bond cleavage is observed.[8,15,16] It is not understood precisely how the nature of the nucleophile influences the product distribution in the solvolysis of VX. Possibilities include effects on the kinetics of the initial attack, effects on the equilibria of any intermediates, and effects on the thermodynamics of the overall reaction.

In trigonal bipyramidal phosphorus compounds, the most electronegative groups generally thermodynamically prefer the apical positions,[23] although exceptions have been noted.[24] Elimination is also more facile from an apical position; thus, the most electronegative group may be expected to be the preferred leaving group in the absence of mitigating factors. Alkoxides are more electronegative than thiolates and are therefore more apicophilic,[25] yet thiolates are less basic and are therefore better leaving groups.[14] An a priori prediction of whether P−O or P−S bond cleavage should dominate becomes an exercise in balance between apicophilicity and leaving group stability. In the case of VX, the thiolate group is the dominant leaving group in the reaction with both hydroxide and hydroperoxide. Other phosphonothiolates display similar results. DeBruin et al. have studied the nucleophilic reaction of *O,S*-dimethyl phenylphosphonothiolate with ethoxide and find a 3:1 preference for displacement of methylthiolate over displacement of methoxide.[26] Yang has reported[15,16] on the alkaline hydrolysis of *O,S*-diethyl methylphosphonothiolate and *O,S*-diethyl phenylphosphonothiolate, finding a pOH-dependent preference for P−S cleavage ranging from 5:1 to 1.5:1 in the first case and 7:1 to 2:1 in the second case. Berg et al. examined a series of *O,S*-dialkyl phenylphosphonothiolates, noting P−S/P−O bond cleavage ratios in the range of 4:1 for diethyl to 1:1 for dimethyl.[27] Jaeger and Li have demonstrated that *O*-methyl *S*-benzyl phenylphosphonothiolate behaves in a very similar fashion.[28]

In the case of *O,S*-dimethyl phenylphosphonothiolate, the authors explained the 3:1 preference for P−S bond cleavage by invoking a slight kinetic preference for the thiolate ligand to be apical at the expense of the methoxide ligand.[26] This translates to a kinetic preference for attack of the nucleophile opposite ethylthiolate, counter to the expected behavior that would place the methoxide ligand preferentially in an apical position. However, the authors were careful to make the point that their explanation may be valid for only the specific phosphonothiolate studied and that a continuum of possible mechanisms is likely to exist dependent upon the substituents on phosphorus and the nucleophile used.

For VX and **1c**, Yang et al. have suggested[16,18] a kinetic preference for an apical alkoxide ligand, contradictory to the findings of DeBruin et al.[26] This conclusion is based upon the observation that the relative yield of **3b/c** to **4b/c** increases with temperature,[16,18] indicating that **4b/c** is the kinetically favored product, while **3b/c** is thermodynamically favored. Unfortunately, the activation energies for P−S and P−O bond cleavage in the alkaline hydrolysis of VX are nearly identical (14.5 and 14.6 kcal/mol),[18] and therefore, the authors are unable to provide additional support for the supposition that having the alkoxy ligand apical is kinetically preferred in the alkaline hydrolysis of VX.

It is, of course, possible that mechanisms other than that shown in Scheme 1 are operative in these reactions. Additional mechanisms that have been proposed for the reaction of VX with hydroperoxide include intramolecular oxygen transfer in the trigonal bipyramidal intermediate following hydroperoxide attack,[15] oxidation of VX to the *N*-oxide followed by hydrolysis[22] or an apparent Cope elimination,[17,22] and oxidation of VX to the *S*-oxide followed by rapid hydrolysis via an addition−elimination mechanism, perhaps with further oxidation at the nitrogen.[17,22] A concerted $S_N2(P)$ mechanism has also been suggested for the perhydrolysis of VX and related compounds.[29] The study of the oxidative mechanisms is outside the scope of the current manuscript but is the subject of other work currently underway. Photocatalytic destruction,[30,31] metal-catalyzed decomposition,[32−36] enzymatic degradation,[37−43] and reduction[44,45] of chemical warfare agents and related molecules have also been studied.

Computational methods offer the ability to explore mechanistic details of these reactions while avoiding exposure to these deadly agents. Both sarin[13] and a model VX compound[46] have been previously examined via ab initio molecular orbital theory; however, neither work provided a direct comparison of the reactivity of these two agents nor a direct comparison of alkaline hydrolysis

(23) Thatcher, G. R. J.; Kluger, R. *Adv. Phys. Org. Chem.* **1989**, *25*, 99.
(24) Cramer, C. J.; Gustafson, S. M. *J. Am. Chem. Soc.* **1993**, *115*, 9315−9316.
(25) Cavell, R. G.; Gibson, J. A.; The, K. I. *Inorg. Chem.* **1978**, *17*, 2880−2885.
(26) DeBruin, K. E.; Tang, C.-l. W.; Johnson, D. M.; Wilde, R. L. *J. Am. Chem. Soc.* **1989**, *111*, 5871−5879.
(27) Berg, F. J.; Moss, R. A.; Yang, Y.-C.; Zhang, H. *Langmuir* **1995**, *11*, 411−413.
(28) Jaeger, D. A.; Li, B. *Langmuir* **2000**, *16*, 5−10.
(29) Yang, Y.-C.; Berg, F. J.; Szafraniec, L. L.; Beaudry, W. T.; Bunton, C. A.; Kumar, A. *J. Chem. Soc., Perkin Trans. 2* **1997**, 607−613.
(30) Vorontsov, A. V.; Davydov, L.; Reddy, E. P.; Lion, C.; Savinov, E. N.; Smitniotis, P. G. *New J. Chem.* **2002**, *26*, 732−744.
(31) Vorontsov, A. V.; Chen, Y.-C.; Smirniotis, P. G. *J. Hazard. Mater.* **2004**, *B113*, 89−95.
(32) Michalkova, A.; Gorb, L.; Ilchenko, M.; Zhikol, O. A.; Shishkin, O. V.; Leszczynski, J. *J. Phys. Chem. B* **2004**, *108*, 1918−1930.
(33) Michalkova, A.; Ilchenko, M.; Gorb, L.; Leszczynski, J. *J. Phys. Chem. B* **2004**, *108*, 5294−5303.
(34) Wagner, G. W.; Bartram, P. W.; Koper, O.; Klabunde, K. J. *J. Phys. Chem. B* **1999**, *103*, 3225−3228.
(35) Tsang, J.; Neverov, A. A.; Brown, R. S. *J. Am. Chem. Soc.* **2003**, *125*, 7602−7607.
(36) Keizer, T. S.; De Pue, L. J.; Parkin, S.; Atwood, D. A. *J. Am. Chem. Soc.* **2002**, *124*, 1864−1865.
(37) Hill, C. M.; Li, W.-S.; Thoden, J. B.; Holden, H. M.; Raushel, F. M. *J. Am. Chem. Soc.* **2003**, *125*, 8990−8991.
(38) Gopal, S.; Rastogi, V.; Ashman, W.; Mulbury, W. *Biochem. Biophys. Res. Commun.* **2000**, *279*, 516−519.
(39) Koca, J.; Zhan, C.-G.; Rittenhouse, R. C.; Ornstein, R. L. *J. Am. Chem. Soc.* **2001**, *123*, 817−826.
(40) Kolakowski, J. E.; J., D. J.; Harvey, S. P.; Szafraniec, L. L.; Beaudry, W. T.; Lai, K.; Wild, J. R. *Biocatal. Biotransform.* **1997**, *15*, 297−312.
(41) Rastogi, V. K.; DeFrank, J. J.; Cheng, T.-C.; Wild, J. R. *Biochem. Biophys. Res. Commun.* **1997**, *241*, 294−296.
(42) Ordentlich, A.; Dov, B.; Sod-Moriah, G.; Kaplan, D.; Mizrahi, D.; Segall, Y.; Kronman, C.; Karton, Y.; Lazar, A.; Marcus, D.; Velan, B.; Shafferman, A. *Biochemistry* **2004**, *43*, 11255−11265.
(43) Amitai, G.; Adani, R.; Hershkovitz, M.; Bel, P.; Rabinovitz, I.; Meshulam, H. *J. Appl. Toxicol.* **2003**, *23*, 225−233.
(44) Kiddle, J. J.; Mezyk, S. P. *J. Phys. Chem. B* **2004**, *108*, 9568−9570.
(45) Aguila, A.; O'Shea, K. E.; Tobien, T.; Asmus, K.-D. *J. Phys. Chem. A* **2001**, *105*, 7834−7839.
(46) Patterson, E. V.; Cramer, C. J. *J. Phys. Org. Chem.* **1998**, *11*, 232−240.

versus perhydrolysis. The goal of this work is 2-fold. First, we reexamine the alkaline hydrolysis of sarin using a variety of common ab initio and density functional methods. Since the alkaline hydrolysis of sarin has been well-studied, this provides an opportunity to benchmark appropriate methods for use on related systems. In particular, we hope to find a method that balances computational efficiency with reasonable accuracy. Second, we provide the first detailed theoretical examination of the solvolysis of a VX-like compound and offer comparisons between alkaline hydrolysis and perhydrolysis. Given the size of VX, we have employed an analogue (*O*,*S*-dimethyl methylphosphonothiolate, **1c**) in order to reduce the required computational time. Model compounds such as **1c** have been shown to have nearly identical solvolysis[15,26] chemistry as VX. The results presented here serve to elucidate questions regarding competing P−O and P−S bond cleavage in these reactions.

Computational Methods

Optimized geometries and harmonic frequencies were obtained using Hartree−Fock and various density functional methods. The density functionals used employed the pure[47] and hybrid[48] exchange functionals of Becke coupled with the correlation functional of Lee, Yang, and Parr[49] (BLYP and B3LYP), the modified one-parameter functional of Perdew and Wang (mPW1PW91),[50,51] a variation thereof developed by the Truhlar group (mPW1K),[52] and a modified functional formed from Becke's one-parameter exchange and kinetic-energy-dependent correlation functionals,[53] also due to the Truhlar group (BB1K).[54] Four basis sets were used in conjunction with the methods listed above: MIDI!,[55] 3-21+G*, 6-31+G(d), and 6-31+G(d,p).[56] The first in the list was developed by the Cramer and Truhlar groups to provide accurate geometries of, inter alia, phosphorus- and sulfur-containing compounds, while the last in the list has been recognized as one of the best double-ζ basis sets available.[57] Electronic energies from these calculations were converted to thermodynamic data based on frequency calculations. Due to concerns over the quality of the entropy terms due to low-frequency vibrations, energies are corrected only to unscaled enthalpies at 298 K.

Given that these molecules have many internal degrees of freedom, some care was taken to find low energy rotational conformers (data not shown). However, we cannot claim that the entire conformational space was sampled in any case. The lowest energy conformers found were used to construct the potential energy surfaces presented. Intrinsic reaction coordinate (IRC) calculations[58] were performed to ascertain the nature of each transition state.

It is well-known that Hartree−Fock theory does not adequately predict barrier heights, and density functional theory (DFT) has been known to underestimate barrier heights.[52,59] Therefore, single-point energies were computed on optimized geometries using second-order Møller−Plesset theory (MP2)[60] and the 6-31+G(d) basis set. The effect of aqueous solvation was accounted for through the use of the integral equation formalism polarized continuum solvation model (IEF-PCM).[61] Single-point IEF-PCM calculations were performed on optimized geometries using both the level of theory at which they were optimized (hereafter, ΔG_{solv1}) and the HF/6-31+G(d) level (hereafter, ΔG_{solv2}).

All calculations were performed using Gaussian 03.[62]

Results and Discussion

For the purposes of this discussion, a level of theory (e.g., HF/MIDI!) indicates that the electronic energy has been corrected to an enthalpy at 298 K. Since the MP2 method was used only with the 6-31+G(d) basis set, "MP2" is taken to mean "MP2/6-31+G(d)". Therefore, a composite level of theory (e.g., MP2//HF/MIDI!) indicates that the reported energy is E(MP2) using the 6-31+G(d) basis set plus the enthalpic correction. Given that all of the chemistry discussed occurs in aqueous solution, all discussion will concern energies that include a correction for the free energy of solvation (e.g., MP2//HF/MIDI! + ΔG_{solv2}). Relative energies are summarized in the following tables for only selected levels of theory. The complete set of data is available in the Supporting Information.

Benchmarking of Methods. In other studies of phosphate ester hydrolysis, it has been shown that using gas-phase optimized structures with single-point solvation energy corrections yields very similar potential energy surfaces as full optimization in solution.[63] It has also been shown for closely related compounds that gas-phase geometries and solvation corrections are relatively insensitive to electron correlation effects but that correlation effects are important for obtaining accurate electronic energies.[64−67] These same studies show that relative electronic energies at the MP2 level closely match those computed at much higher levels of theory. We therefore expect that our methods will also accurately model the experimental aqueous process.

(47) Becke, A. D. *Phys. Rev. A* **1988**, *38*, 3098−3100.
(48) Becke, A. D. *J. Chem. Phys.* **1993**, *98*, 5648−5652.
(49) Lee, C.; Yang, W.; Parr, R. G. *Phys. Rev. B* **1988**, *37*, 785−789.
(50) Adamo, C.; Barone, V. *J. Chem. Phys.* **1998**, *108*, 664−675.
(51) Perdew, J. P.; Chevary, J. A.; Vosko, S. H.; Jackson, K. A.; Pederson, M. R.; Singh, D. J.; Fiolhais, C. *Phys. Rev. B* **1992**, *46*, 6671−6687.
(52) Lynch, B. J.; Truhlar, D. G. *J. Phys. Chem. A* **2001**, *105*, 2936−2941.
(53) Becke, A. D. *J. Chem. Phys.* **1996**, *104*, 1040−1046.
(54) Zhao, Y.; Lynch, B. J.; Truhlar, D. G. *J. Phys. Chem. A* **2004**, *108*, 2715−2719.
(55) Easton, R. E.; Giesen, D. J.; Welch, A.; Cramer, C. J.; Truhlar, D. G. *Theor. Chem. Acc.* **1996**, *93*, 281−301.
(56) Hehre, W. J.; Radom, L.; Schleyer, P. v. P.; Pople, J. A. *Ab Initio Molecular Orbital Theory*; Wiley: New York, 1986.
(57) Zhao, Y.; Pu, J.; Lynch, B. J.; Truhlar, D. G. *Phys. Chem. Chem. Phys.* **2004**, *6*, 673−676.
(58) Gonzales, C.; Schlegel, H. B. *J. Chem. Phys.* **1989**, *90*, 2154.
(59) Baker, J.; Muir, M.; Andzelm, J. *J. Chem. Phys.* **1995**, *102*, 2063−2079.
(60) Møller, C.; Plesset, M. S. *Phys. Rev.* **1934**, *46*, 618−622.
(61) Cances, E.; Mennucci, B.; Tomasi, J. *J. Chem. Phys.* **1997**, *107*, 3032−3041.
(62) Frisch, M. J.; Trucks, G. W.; Schlegel, H. B.; Scuseria, G. E.; Robb, M. A.; Cheeseman, J. R.; Jr., J. A. M.; Vreven, T.; Kudin, K. N.; Burant, J. C.; Millam, J. M.; Iyengar, S. S.; Tomasi, J.; Barone, V.; Mennucci, B.; Cossi, M.; Scalmani, G.; Rega, N.; Petersson, G. A.; Nakatsuji, H.; Hada, M.; Ehara, M.; Toyota, K.; Fukuda, R.; Hasegawa, J.; Ishida, M.; Nakajima, T.; Honda, Y.; Kitao, O.; Nakai, H.; Klene, M.; Li, X.; Knox, J. E.; Hratchian, H. P.; Cross, J. B.; Bakken, V.; Adamo, C.; Jaramillo, J.; Gomperts, R.; Stratmann, R. E.; Yazyev, O.; Austin, A. J.; Cammi, R.; Pomelli, C.; Ochterski, J. W.; Ayala, P. Y.; Morokuma, K.; Voth, G. A.; Salvador, P.; Dannenberg, J. J.; Zakrzewski, V. G.; Dapprich, S.; Daniels, A. D.; Strain, M. C.; Farkas, O.; Malick, D. K.; Rabuck, A. D.; Raghavachari, K.; Foresman, J. B.; Ortiz, J. V.; Cui, Q.; Baboul, A. G.; Clifford, S.; Cioslowski, J.; Stefanov, B. B.; Liu, G.; Liashenko, A.; Piskorz, P.; Komaromi, I.; Martin, R. L.; Fox, D. J.; Keith, T.; Al-Laham, M. A.; Peng, C. Y.; Nanayakkara, A.; Challacombe, M.; Gill, P. M. W.; Johnson, B.; Chen, W.; Wong, M. W.; Gonzalez, C.; Pople, J. A. *Gaussian 03*, Revision C.2; Gaussian, Inc.: Wallingford CT, 2004
(63) Florian, J.; Warshel, A. *J. Phys. Chem. B* **1998**, *102*, 719−734.
(64) Xiong, Y.; Zhan, C.-G. *J. Org. Chem.* **2004**, *69*, 8451−8458.
(65) Zhan, C.-G.; Landry, D. W.; Ornstein, R. L. *J. Am. Chem. Soc.* **2000**, *122*, 1522−1530.
(66) Zhan, C.-G.; Landry, D. W.; Ornstein, R. L. *J. Phys. Chem. A* **2000**, *104*, 7672−7678.
(67) Zhan, C.-G.; Landry, D. W.; Ornstein, R. L. *J. Am. Chem. Soc.* **2000**, *122*, 2621−2627.

TABLE 1. Computed Enthalpies of Activation and Error with Respect to Experiment for the Best Performing Levels of Theory for the Alkaline Hydrolysis of Sarin

level of theory	computed $\Delta H^{\ddagger}$ (kcal/mol)	Error1[a] (kcal/mol)	Error2[b] (kcal/mol)	average error (kcal/mol)
MP2//BLYP/MIDI! + ΔG_{solv2}	10.57	2.07	0.57	1.32
MP2//HF/MIDI! + ΔG_{solv2}	8.10	−0.40	−1.90	−1.15
MP2//mPW1K/MIDI! + ΔG_{solv2}	10.16	1.66	0.16	0.91
HF/6-31+G(d,p) + ΔG_{solv2}	10.16	1.66	0.16	0.91
HF/6-31+G(d,p) + ΔG_{solv1}	9.98	1.48	−0.02	0.73
MP2//HF/MIDI! + ΔG_{solv1}	9.96	1.46	−0.04	0.71
HF/6-31+G(d) + ΔG_{solv1}	9.90	1.40	−0.10	0.65
Exp1[c]	8.5			
Exp2[d]	10.0			

[a] Absolute error relative to Exp1. [b] Absolute error relative to Exp2. [c] From ref 11. [d] From ref 12.

We first compare our computed activation enthalpies for the alkaline hydrolysis of sarin with the two available activation barriers. We have converted the Arrhenius activation barrier of Larsson to an enthalpy of activation for the purposes of this comparison.[68] Examination of the data for alkaline hydrolysis of sarin reveals that only a handful of the tested combinations reproduce both the experimental enthalpies of activation within ca. 2 kcal/mol. These methods are listed in Table 1.

Interestingly, the majority of the methods that work well employ the MIDI! basis set for geometry optimization. This is perhaps not surprising, as the MIDI! basis set was developed to provide geometries and charges comparable to MP2/cc-pVDZ for H-, C-, N-, O-, F-, P-, S-, and Cl-containing molecules.[55] MIDI! was not, however, designed to provide good relative energies, and it is clear from Table 1 that the MP2 single-point energy is essential in order to get good agreement with experiment. It is also interesting to note that most of the methods agree better with the activation enthalpy determined by Gustafson and Martell. Theirs is the more recent study and was conducted over a slightly broader range of temperature and pH conditions than the study of Larsson. However, it is difficult to determine which experimental value is more accurate, and it is perhaps best to consider the average error as a better measure of a method's performance. On this basis, all of the methods listed in Table 1 predict the enthalpy of activation with reasonable accuracy and might be chosen for similar studies.

As one of our goals is to find an accurate method that is computationally efficient, we have focused on the methods that employ the small MIDI! basis set. Optimizations at the HF/MIDI!, BLYP/MIDI!, and mPW1K/MIDI! levels all gave satisfactory results for the alkaline hydrolysis of sarin. However, it is well-known that HF theory may not adequately describe molecules with peroxide moieties, such as the structures necessary to study the perhydrolysis reactions presented here.[69] Both pure and hybrid density functionals have been used for the study of peroxides with some success, and hybrid functionals perform better than pure functionals.[70] Furthermore, the mPW1K hybrid functional has been developed specifically for accurate estimation of barrier heights.[52] Taking each of these caveats into account, we will focus the following discussion on geometries obtained at the mPW1K/MIDI! level of theory, while additional data for the HF/MIDI! and BLYP/MIDI! geometries may be found in the Supporting Information.

Alkaline Hydrolysis of Sarin. Geometries of the organophosphorus species involved in the alkaline hydrolysis of sarin are depicted in Figure 1. Absolute energies are presented in Table 2, while the potential energy surface is given in Figure 2.

The potential energy surface computed for the alkaline hydrolysis of sarin at the MP2//mPW1K/MIDI! + ΔG_{solv2} level of theory is completely consistent with the accepted addition−elimination pathway (Scheme 1). The transition state for hydroxide attack (**TS1a**) lies 10.2 kcal/mol above separated reactants, in good agreement with the available experimental data.[11,12] The transition state has a P−OH bond distance of 2.845 Å, and the hydroxide approaches the backside of the fluoride in a slightly nonlinear fashion (O−P−F angle 166.2°). Significant stabilizing hydrogen-bonding interactions can be seen between the nucleophile and the ligands on sarin (Figure 1).

Trigonal bipyramidal intermediate **2a1**, with the isopropyl group oriented to stabilize the hydroxide, is found to lie 22.0 kcal/mol below **TS1a**, or 11.8 kcal/mol below separated reactants. The P−F distance has increased to 1.687 Å while the P−OH distance has closed to 1.777 Å. The O−P−F angle deviates from linearity by less than 10° (171.1°). A second trigonal bipyramid, **2a2**, is found where the isopropyl group is oriented toward the fluoride. This trigonal bipyramid is 1.4 kcal/mol lower in energy than **2a1**, and the enthalpy of activation for the interconversion of **2a1** to **2a2** is 2.1 kcal/mol.

The transition state for loss of fluoride (**TS2a**) is found to lie only 0.3 kcal/mol above **2a2**. The P−F bond is stretched to 3.027 Å, indicating a somewhat late transition state. Significant hydrogen bonding to the methyl and isopropyl ligands has pulled the fluoride significantly off a linear trajectory (O−P−F angle 155.6°). The final point in our potential energy surface is phosphonate **3a** plus hydrogen fluoride.[71] The separated products lie 17.9 kcal/mol below **TS2a**, or 30.8 kcal/mol below separated reactants. The computed stationary points and accom-

(68) Based on the relationship $E_a = \Delta H^{\ddagger} + RT$, at 298 K.

(69) See, for example, the discussion in: Cramer, C. J. *Essentials of Computational Chemistry: Theories and Models*, 2nd ed.; John Wiley and Sons Ltd: West Sussex, England, 2004.

(70) Jursic, B. S.; Martin, R. M. *Int. J. Quantum Chem.* **1996**, *59*, 495−501.

(71) It should be noted that while TS2a proceeds to the phosphonic acid product, comparison with experiment requires the phosphonate anion. Therefore, we report as "final products" data for the anionic organophosphorus products and neutral leaving groups (hydrogen fluoride, methanol, or methanethiol) in this and every other reaction.

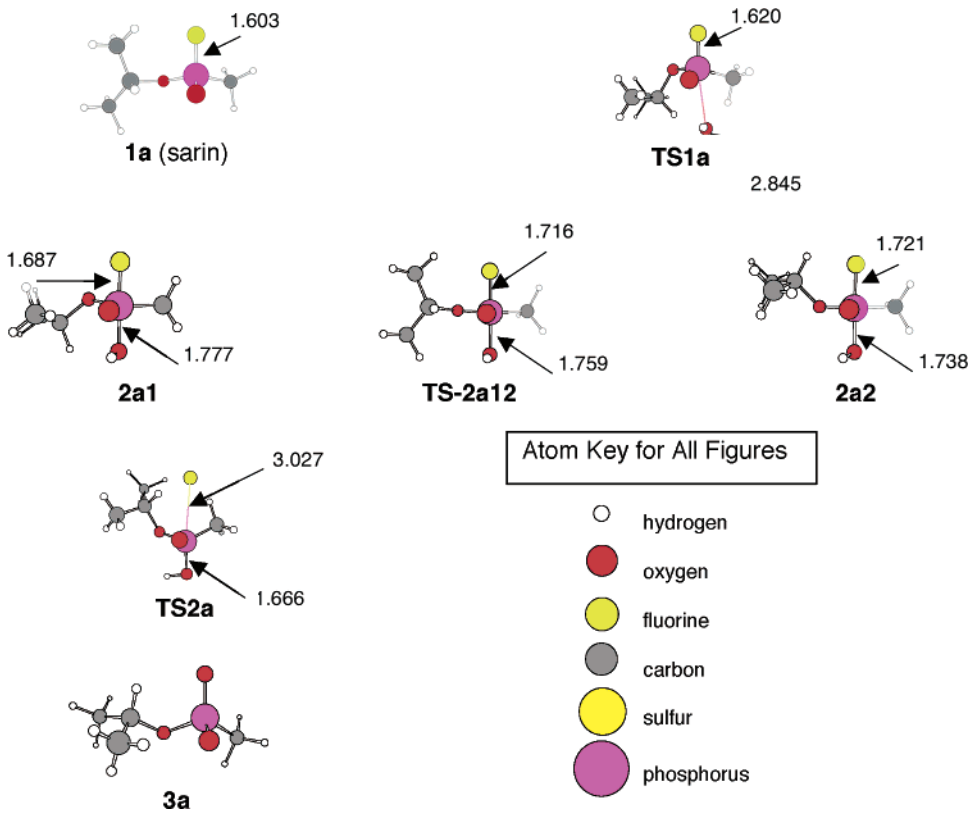

FIGURE 1. Geometries optimized at the mPW1K/MIDI! level for the organophosphorus species involved in the alkaline hydrolysis of sarin. Selected bond distances (Å) are indicated.

TABLE 2. Relevant Energies for the Reaction of Hydroxide with Sarin

	E(SCF)[a]	$H_{298} - H_0$[a,b]	E(MP2)[c]	ΔG_{solv2}[d]
sarin (**1a**)	−746.06396	0.16071	−748.47908	2.2
hydroxide	−75.22178	0.01054	−75.58201	−86.4
TS1a	−821.41479	0.17109	−824.10013	−49.5
2a1	−821.45912	0.17579	−824.13539	−52.2
TS-2a1to2	−821.45447	0.17470	−824.13147	−51.9
2a2	−821.45799	0.17561	−824.13687	−52.7
TS2a	−821.41855	0.17189	−824.12416	−57.9
3a	−721.60161	0.15976	−723.94516	−54.9
HF	−99.82305	0.01249	−100.19986	−8.0

[a] At the mPW1K/MIDI! level, in units of hartrees. [b] Includes unscaled zero-point vibrational energy. [c] At the MP2/6-31+G(d)//mPW1K/MIDI! level, in units of hartrees. [d] At the HF/6-31+G(d)//mPW1K/MIDI! level, in units of kcal/mol.

panying IRC calculations indicate that this is, in fact, a two-step addition−elimination mechanism. However, the relative energies reveal a reaction profile that is more similar to a concerted reaction, with the first step being the rate-determining step while the ensuing steps are very rapid by comparison.

Zheng et al. have reported on the same reaction at the MP2/6-31+G(d)//HF/6-31+G(d) level, with solvent effects accounted for via a local implementation of the surface and volume polarizations for electrostatics (SVPE) model.[13] It is important to note that the energies reported herein contain enthalpic corrections to 298 K whereas the energies reported by Zheng et al. contain only zero-point energy corrections. Agreement between the two studies is good, with gross structural features being comparable. The energetics are also similar, with our barrier for hydroxide attack being higher (10.2 kcal/mol vs 8.6 kcal/mol) while our barrier for fluoride loss is identical (0.3 kcal/mol).

This disagreement in the hydroxide attack barrier can be rationalized by considering the most significant difference in methodology. The SVPE solvation model[72−74] used by Zheng et al. employs a scheme to accurately determine both surface and volume polarizations self-consistently. This may be seen as superior to the way the IEF-PCM solvation model estimates volume polarization. In a study of ester hydrolysis, results employing the SVPE model were found to give better agreement with experiment than results employing the IEF-PCM model.[66] The IEF-PCM results consistently overestimated the reaction barriers by 1−4 kcal/mol, depending on the size of the ester, with smaller esters giving smaller errors. The comparison of our current work with the previous work of Zheng et al., as well as other work by Chen and Zhan on ester hydrolysis,[75,76] suggests that IEF-PCM will generally overestimate reaction barriers relative to SVPE. However, since SVPE is not yet generally available, the IEF-PCM model presents itself as a worthy alternative.

Solvolysis of VX Model Compound *O*,*S*-Dimethyl Methylphosphonothiolate (1c). Using the MP2//mPW1K/MIDI! + ΔG_{solv2} level of theory, we have computed detailed addition−elimination pathways for the

(72) Zhan, C.-G.; Bentley, J.; Chipman, D. M. *J. Chem. Phys.* **1998**, *108*, 177−192.
(73) Zhan, C.-G.; Chipman, D. M. *J. Chem. Phys.* **1998**, *109*, 10543−10558.
(74) Zhan, C.-G.; Chipman, D. M. *J. Chem. Phys.* **1999**, *110*, 1611−1622.
(75) Chen, X.; Zhan, C.-G. *J. Phys. Chem. A* **2004**, *108*, 3789−3797.
(76) Chen, X.; Zhan, C.-G. *J. Phys. Chem. A* **2004**, *108*, 6407−6413.

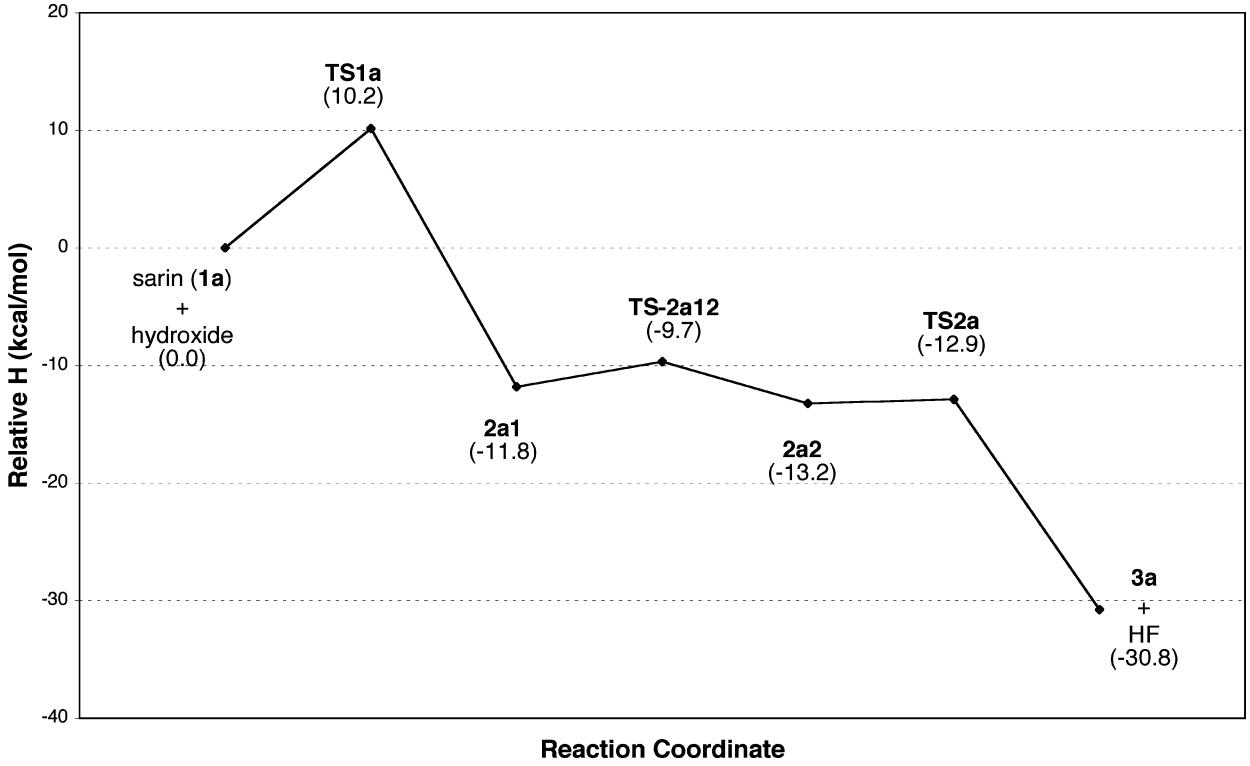

FIGURE 2. Potential energy surface for the alkaline hydrolysis of sarin at the MP2//mPW1K/MIDI! + ΔG_{solv2} level of theory.

TABLE 3. Relevant Energies for the Reaction of Hydroxide with VX Model 1c

	E(SCF)[a]	$H_{298} - H_0$[a,b]	E(MP2)[c]	ΔG_{solv2}[d]
1c	−1004.57942	0.14049	−1007.86602	2.3
hydroxide	−75.22178	0.01054	−75.58769	−86.7
TS1c	−1079.92306	0.15133	−1083.47693	−50.9
TS1d	−1079.92836	0.15049	−1083.48228	−51.2
2c1	−1079.96976	0.15531	−1083.51688	−50.8
TS-2c12	−1079.96801	0.15419	−1083.51550	−48.7
2c2	−1079.97039	0.15539	−1083.51786	−50.3
2d1	−1079.97390	0.15507	−1083.52052	−47.4
TS-2d12	−1079.95549	0.15405	−1083.50754	−48.8
2d2	−1079.97103	0.15503	−1083.52124	−50.3
TS2c	−1079.96383	0.15424	−1083.52019	−52.3
TS2d	−1079.93705	0.15090	−1083.49110	−51.3
TSrot-dc	−1079.95529	0.15424	−1083.50411	−46.2
3c	−643.43665	0.09901	−645.59778	−60.4
methanethiol	−436.53672	0.05223	−437.95559	0.2
4c	−964.95642	0.09652	−968.18828	−57.3
methanol	−115.01256	0.05681	−115.35735	−2.4

[a] At the mPW1K/MIDI! level, in units of hartrees. [b] Includes unscaled zero-point vibrational energy. [c] At the MP2/6-31+G(d)//mPW1K/MIDI! level, in units of hartrees. [d] At the HF/6-31+G(d)//mPW1K/MIDI! level, in units of kcal/mol.

attack of both hydroxide and hydroperoxide on VX model compound **1c**. Scheme 1 now becomes slightly more complicated than shown, as there are four total trigonal bipyramidal intermediates of interest: **2c**, with OH and SCH_3 apical, **2d**, with OH and OCH_3 apical, and **2e** and **2f**, which are analogous to **2c** and **2d**, except with OOH in place of OH, and each of these has two rotamers of interest (e.g., **2c1** and **2c2**). There are, then, 12 total transition states of interest, one each for formation and dissociation of the four trigonal bipyramids, and one for interconversion of each rotamer pair. Table 3 and Figures 3 and 4 report the relevant data for hydroxide attack, while Table 4 and Figures 5 and 6 report the relevant data for hydroperoxide attack.

Alkaline Hydrolysis of *O*,*S*-Dimethyl Methylphosphonothiolate (1c). An examination of the geometries presented in Figures 1 and 3 shows that there are few significant differences between sarin and **1c** when attacked by hydroxide. Attack of hydroxide opposite methylthiolate leads through **TS1c** to trigonal bipyramid **2c1**, and the activation enthalpy for this attack is 18.8 kcal/mol. Intermediate **2c1** can then rotate to trigonal bipyramid **2c2** with a modest activation enthalpy of 2.3 kcal/mol. The two trigonal bipyramidal intermediates are essentially isoenergetic, lying 3.7 and 3.8 kcal/mol below separated reactants, respectively. Once **2c2** is formed, the process of P−S bond cleavage is barrierless. The final products of hydroxide attack opposite methylthiolate lie 38.5 kcal/mol below separated reactants.

Despite the fact that **TS2c** is confirmed by IRC calculations to lead from **2c2**, a negative activation enthalpy is found. This may be due to the use of gas-phase geometries to construct an approximate solution-phase surface. While the effect of approximating solution-phase phosphate ester hydrolysis potential energy surfaces in this way is believed to be small,[63] it is reasonable to assume that the relative positions of each stationary point, and therefore their relative energies, will shift upon reoptimization in solution. A number of small, additive errors could conceivably lead to the finding of a negative barrier for a process that, in reality, has a modest positive barrier or vice versa.

There is a noticeable difference in both geometries and energies when contrasting attack of hydroxide opposite methoxide with attack opposite methylthiolate. The transition state for attack of hydroxide opposite methoxide (**TS1d**) reveals an activation enthalpy of only 14.6 kcal/mol and is looser than **TS1c**, with P−OH distances of 2.995 and 2.771 Å, respectively. There is a larger

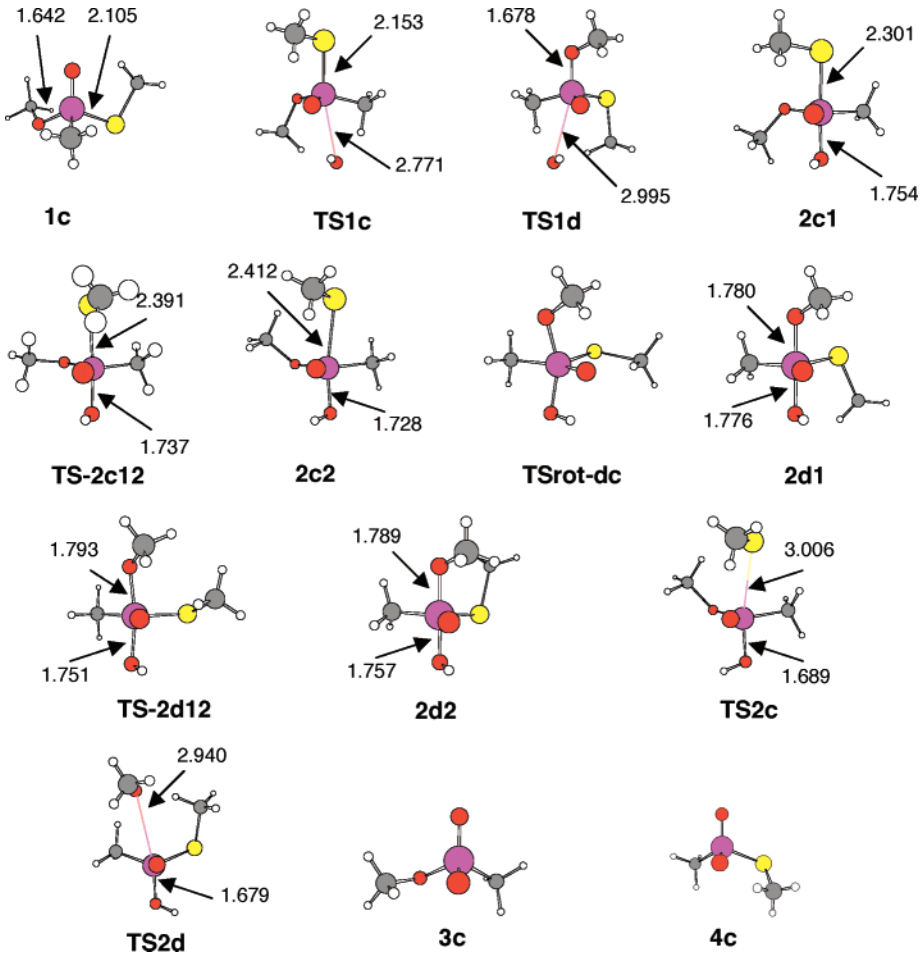

FIGURE 3. Geometries optimized at the mPW1K/MIDI! level for the organophosphorus species involved in the alkaline hydrolysis of VX model **1c**. Selected bond distances (Å) are indicated.

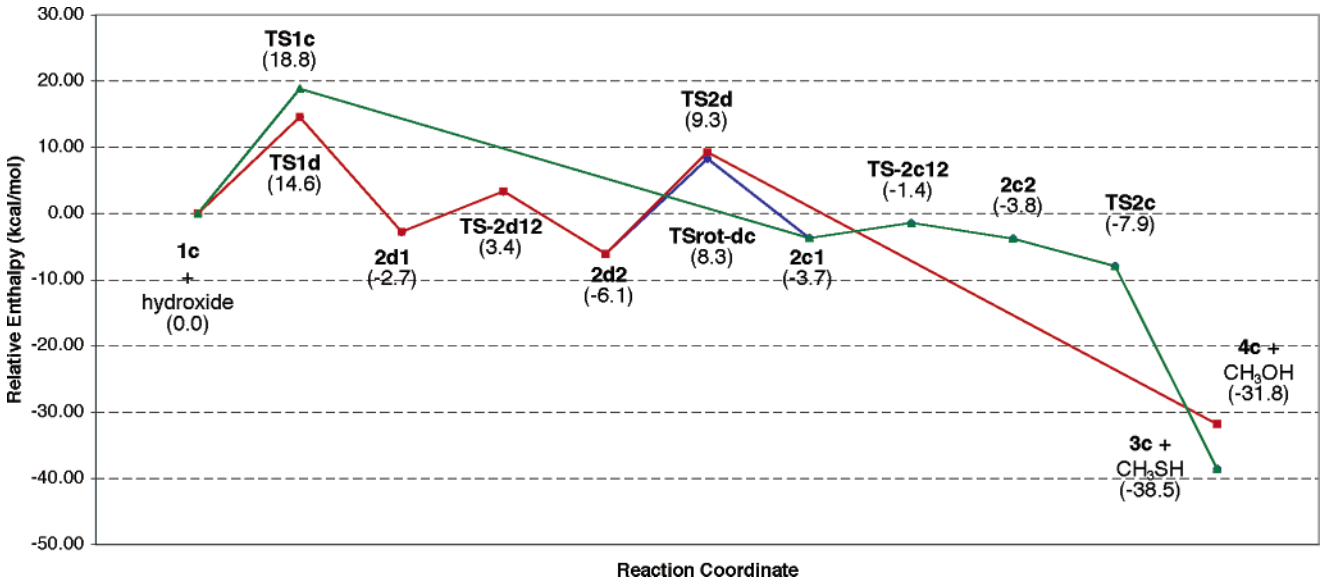

FIGURE 4. Potential energy surface for the alkaline hydrolysis of **1c** at the MP2//mPW1K/MIDI! + ΔG_{solv2} level of theory.

activation enthalpy associated with the interconversion of **2d1** to **2d2** (6.1 kcal/mol) than for **2c1** to **2c2** (2.3 kcal/mol), and **2d2** is more stable than **2d1** by 3.4 kcal/mol. A significant activation enthalpy is found for P−O bond cleavage from **2d2** (15.4 kcal/mol), as opposed to the barrierless P−S cleavage process from **2c2**. The final products for hydroxide attack opposite methoxide lie 31.8 kcal/mol below separated reactants.

The greater degree of bond formation in **TS1c** versus **TS1d**, and the barrierless loss of methylthiolate from

TABLE 4. Relevant Energies for the Reaction of Hydroperoxide with VX Model 1c

	E(SCF)[a]	$H_{298} - H_0$[a,b]	E(MP2)[c]	ΔG_{solv2}[d]
1c	−1004.57942	0.14049	−1007.86602	2.6
hydroperoxide	−149.95075	0.01652	−150.54530	−82.3
TS1e	−1154.62306	0.15664	−1158.43864	−51.1
TS1f	−1154.62698	0.15594	−1158.44244	−52.1
2e1	−1154.67581	0.16082	−1158.47290	−45.6
TS-2e12	−1154.66839	0.15981	−1158.46869	−45.9
2e2	−1154.67097	0.16086	−1158.47175	−46.6
2f1	−1154.67973	0.16058	−1158.48019	−44.4
TS-2f12	−1154.65849	0.15953	−1158.46606	−46.6
2f2	−1154.67197	0.16038	−1158.47613	−47.9
TS2e	−1154.65351	0.15956	−1158.46618	−46.9
TS2f	−1154.62578	0.15533	−1158.43008	−43.5
TSrot-fe	−1154.65748	0.15914	−1158.46124	−43.1
TS-ox	−1154.62501	0.15783	−1158.47166	−48.3
3d	−718.09995	0.10298	−720.51217	−55.5
methanethiol	−436.53672	0.05223	−437.95559	0.2
4d	−1039.61412	0.10034	−1043.10079	−54.4
methanol	−115.01256	0.05681	−115.35735	−2.4
5	−1154.72040	0.15993	−1158.54675	−49.1

[a] At the mPW1K/MIDI! level, in units of hartrees. [b] Includes unscaled zero-point vibrational energy. [c] At the MP2/6-31+G(d)//mPW1K/MIDI! level, in units of hartrees. [d] At the HF/6-31+G(d)//mPW1K/MIDI! level, in units of kcal/mol.

2c2, suggest that attack of hydroxide opposite methylthiolate is nearly a concerted process. This corroborates very nicely the suggestion by DeBruin et al. that nucleophilic attack opposite thiolate ligands in phosphonothiolates is less stepwise than the corresponding attack opposite alkoxide ligands.[26] However, since attack opposite methylthiolate is energetically disfavored in this system, the overall mechanism is still very much a two-step, addition−elimination process (vide infra), which must proceed through trigonal bipyramid **2d1**.

To obtain a more complete picture of the potential energy surface, it is also necessary to consider whether trigonal bipyramid **2d1** (or **2d2**) is easily converted to **2c1** (or **2c2**) via pseudorotation.[77,78] A single pathway involving pseudorotation from **2d1/2** to **2c1/2** was explored (Scheme 3).

The rate-determining step, labeled **TSrot-dc** in Figure 4, is the first pseudorotation with an activation enthalpy of 14.4 kcal/mol, which is only 1 kcal/mol lower than the activation enthalpy for methoxide loss from **2d2**. Of course, it is possible that other pseudorotational pathways are more energetically favorable, but we can at least claim that **2d2** can either undergo P−O bond cleavage or pseudorotation to **2c1** with nearly equal likelihood.

Following a Curtin−Hammett analysis of the entire computed potential energy surface for alkaline hydrolysis of **1c**, a clear picture of the likely mechanism emerges. Attack of hydroxide opposite methoxide is favored by over 1200:1 over attack opposite methylthiolate, indicating that the trigonal bipyramid with the more electronegative ligand apical (**2d1**) is virtually the exclusive product of initial nucleophilic attack. Once **2d1** is formed, it quickly rotates to **2d2**, where the P−O bond cleavage process to form **4c** is competitive with the pseudorotational process to form **2c1**. Any **2c1** formed by pseudorotation will immediately rotate to **2c2** and then cleave the P−S bond in a barrierless fashion to form product **3c**. Therefore, the primary factor determining the ratio of P−S to P−O bond cleavage in the alkaline hydrolysis of **1c** is the competing P−O bond cleavage and pseudorotational processes of **2d2**. The predicted branching ratio based our single pseudorotational pathway is 5:1 in favor of P−S bond cleavage, in excellent agreement with the reported product distributions for the closely related *O,S*-diethyl methylphosphonothiolate, which range from 5:1 to 1.5:1 depending on exact reaction conditions.[16]

Our results agree well with the available experimental data for alkaline hydrolysis of organophosphonothiolates. In the absence of internal or external catalysis, Yang et al. report Arrhenius activation energies of 14.5 and 14.6 kcal/mol for P−S and P−O bond cleavage, respectively, which correspond to activation enthalpies of 13.9 and 14.0 kcal/mol.[68] In our potential energy surface, one of two steps can be taken as the rate-determining step for P−S bond cleavage; initial attack of hydroxide to form **2d1** or pseudorotation of **2d2** to **2c1**, with activation enthalpies of 14.6 and 14.4 kcal/mol, respectively. The rate-determining step for P−O bond cleavage is the actual cleavage from **2d2**, with an enthalpy of activation of 15.4 kcal/mol. While our results are not in exact agreement with the data available for VX, the trends are correct and recent work on phosphonofluoridates indicates that the reaction barrier for alkaline hydrolysis varies according to substitutents by several kcal/mol.[64]

Perhydrolysis of *O,S*-Dimethyl Methylphosphonothiolate (1c). Once again, examination of Figures 1, 3, and 5 reveals few significant differences in geometries across these three reactions. As was the case in alkaline hydrolysis of **1c**, **TS1e** for nucleophilic attack opposite methylthiolate is more compact than **TS1f** for attack opposite methoxide. Converse to the case of hydrolysis, the P−S bond in **TS2e** has stretched significantly (over 1 Å) relative to its value in **2e2**, and there is a noticeable barrier for P−S bond cleavage (2.4 kcal/mol). Nevertheless, reaction of **1c** with either hydroxide or hydroperoxide is less stepwise when the nucleophile attacks opposite methylthiolate than when the nucleophile attacks opposite methoxide.

As in the case of alkaline hydrolysis, attack of the nucleophile opposite the methoxide ligand of **1c** is kinetically preferred, and the trigonal bipyramidal structure with methoxide apical (**2f1**) is more stable than the structure with methylthiolate apical (**2e1**). The rotation of **2f1** to **2f2** has an activation enthalpy of 6.0 kcal/mol, while the conversion of **2e1** to **2e2** requires only 1.7 kcal/mol. Now, the potential energy surface for perhydrolysis deviates significantly from that for alkaline hydrolysis. The barrier for perhydrolytic P−O bond cleavage from **2f2** is 30.2 kcal/mol, while that for pseudorotation to **2e1** through **TSrot-fe** is only 13.4 kcal/mol. This difference is sufficiently large so that P−O bond cleavage cannot possibly compete with pseudorotation and subsequent P−S bond cleavage.

The higher activation enthalpy predicted for **TS2f** compared to the analogous **TS2d** when hydroxide is the nucleophile seems likely to be in part associated with the substantial decrease in exothermicity observed for this pathway when the nucleophile is hydroperoxide. An increase in the activation enthalpy as the reaction goes

(77) Berry, R. S. *J. Chem. Phys.* **1960**, *32*, 933−938.
(78) Mislow, K. *Acc. Chem. Res.* **1970**, *3*, 321−331.

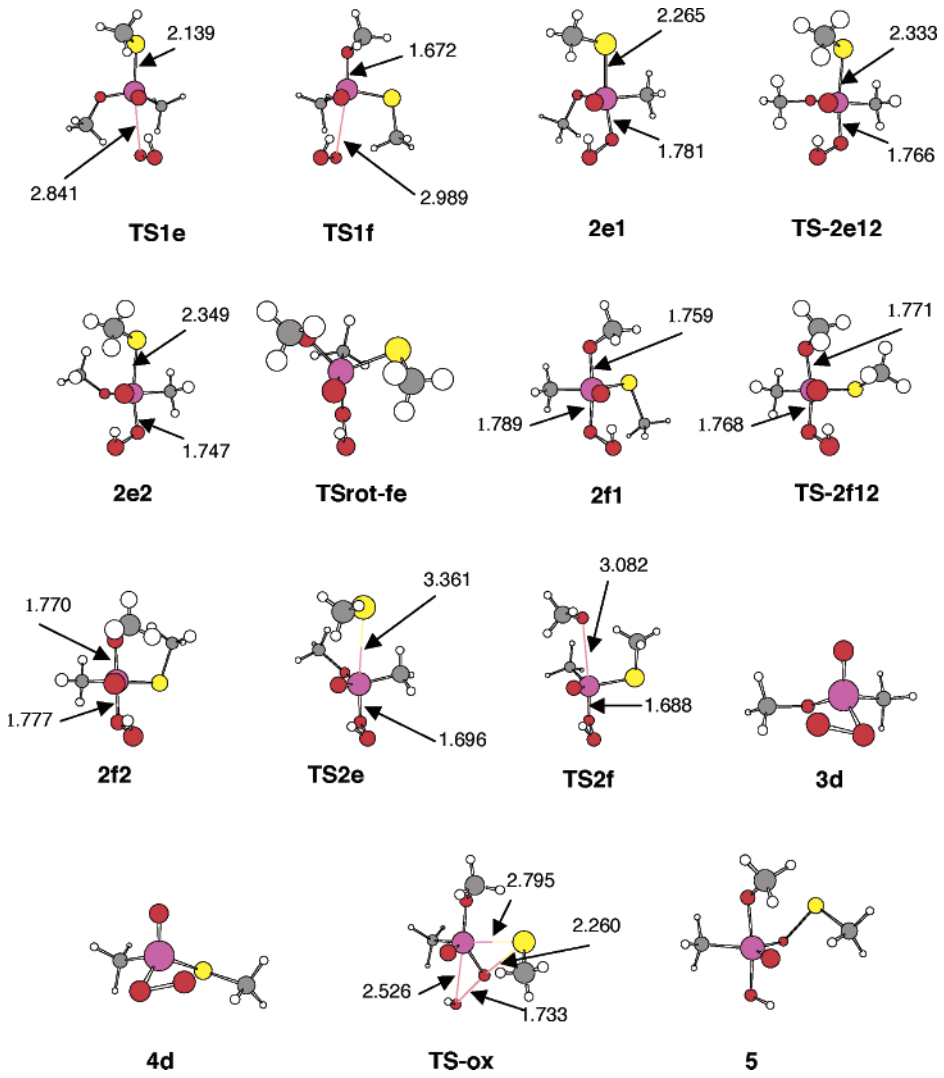

FIGURE 5. Geometries optimized at the mPW1K/MIDI! level for the organophosphorus species involved in the perhydrolysis of VX model **1c**. Selected bond distances (Å) are indicated. The geometry of **1c** is presented in Figure 3.

from highly exothermic to near thermoneutral is consistent with the Hammond postulate.[79] Comparing the processes leading to P−S bond cleavage, the thermochemistry of the pseudorotation that is the rate-determining step is not much affected by the identity of the nucleophile, and hence, the predicted activation barrier is insensitive to the change in net exothermicity.

An alternate fate of trigonal bipyramid **2f1** has been proposed by Yang et al.[15] Intramolecular oxidation at sulfur could yield a phosphinyloxysulfenate,[80] passing through a three-membered ring species as either an intermediate or transition state. Despite the fact that isotopic labeling studies cast doubt on the existence of this pathway,[29] we chose to explore whether it is energetically accessible. Rather than finding a pathway leading to the phosphinyloxylsulfentate, we found a somewhat unusual transition state (**TS-ox)** for the concerted rearrangement of **2f1** to trigonal bipyramidal structure **5** (Scheme 4). This concerted pathway has been confirmed by IRC calculations.

We compute this process to be barrierless, indicating that internal oxidation may in fact be preferred over pseudorotation and thiolate elimination. Presumably, trigonal bipyramid **5** will undergo facile pseudorotation and elimination of the sulfenate, giving phosphonate **3c** as the final organophosphorus product. This process was not explored, and for now we are content to show that this internal oxidation may be possible. A more complete mechanistic survey will be necessary to further clarify this issue.

One important ramification of the concerted nature of the rearrangement from **2f** to **5** is that this pathway cannot be ruled out based on reaction in isotopically labeled water.[29] Since the hydroxide group in **5** is from the original hydroperoxide nucleophile, there is never a second nucleophilic attack and **2f** effectively self-hydrolyses through **5** to give **3c**, without incorporation of isotopically labeled solvent in either **3c** or the leaving group. Yang et al. assumed that internal oxidation of **2f** would yield a phosphinyloxysulfenate, which would then be hydrolyzed by labeled water, and the label would then be detectible in the products. When no label was detected, the internal oxidation pathway was discounted.[29] How-

(79) Hammond, G. S. *J. Am. Chem. Soc.* **1955**, *77*, 334−338.
(80) Segall, Y.; Casida, J. E. *Tetrahedron Lett.* **1982**, *23*, 139−142.

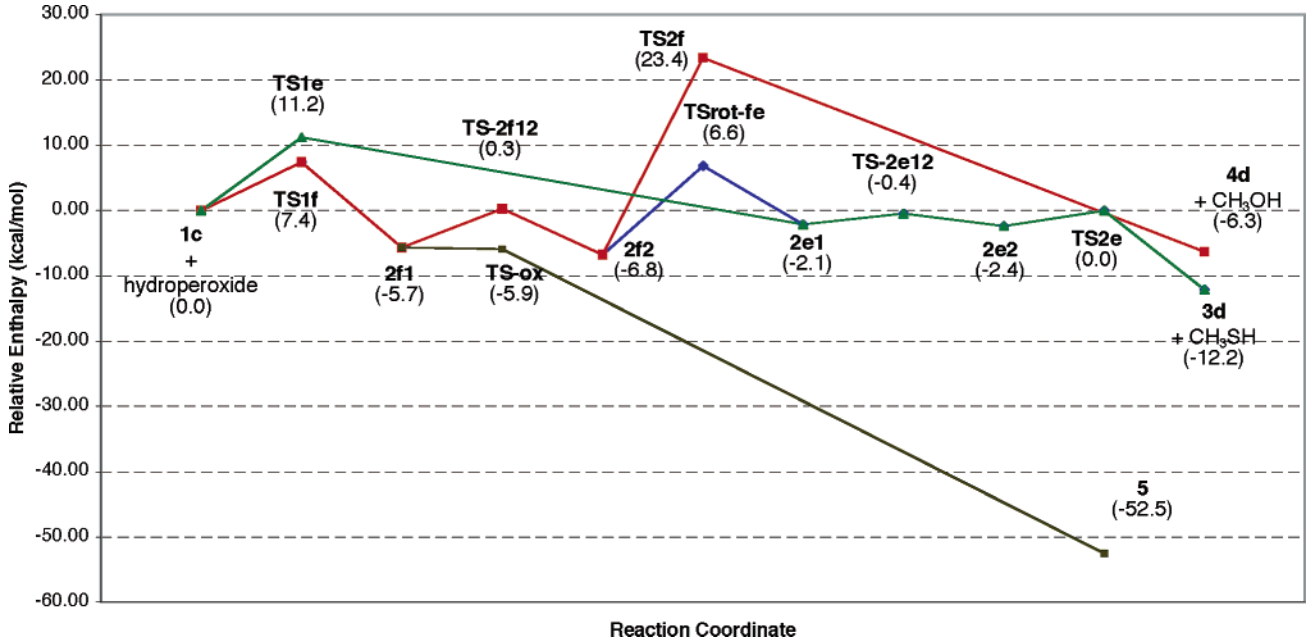

FIGURE 6. Potential energy surface for the perhydrolysis of **1c** at the MP2//mPW1K/MIDI! + ΔG_{solv2} level of theory.

SCHEME 3. Pseudorotational Pathway between Structures 2d/f and 2c/e

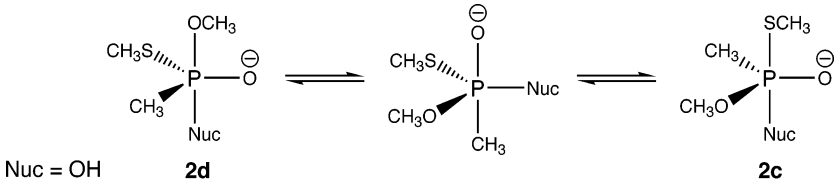

SCHEME 4. Intramolecular Oxidation Pathway from Trigonal Pyramid 2f

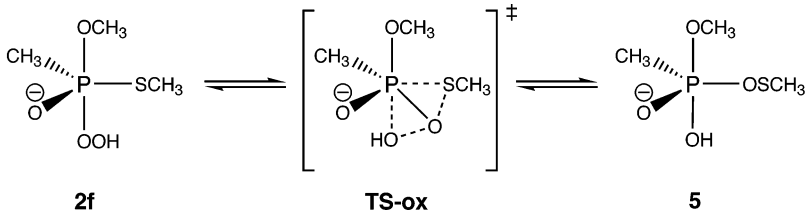

ever, given the mechanism proposed in Scheme 4, there is no need to discount the rearrangement pathway based on labeling evidence alone.

In light of their isotopic labeling study, Yang et al. suggested that preferential P−S bond cleavage in the perhydrolysis of VX and related compounds is best explained by invoking a concerted, $S_N2(P)$ mechanism and argued against alkoxide loss being energetically inaccessible.[29] Our data, however, clearly support a stepwise mechanism where the determining factor is indeed the inability of P−O bond cleavage to compete with P−S bond cleavage. Certainly, it is possible or even likely that the perhydrolysis of *O,S*-dimethyl methylphosphonothiolate (**1c**) follows a slightly different mechanism than VX, *O,S*-diethyl methylphosphonothiolate[29] or *O,S*-dimethyl phenylphosphonothiolate,[26] but for the case of **1c**, it now seems clear that the mechanism is stepwise and that P−O bond cleavage is simply kinetically unfavorable when compared to P−S bond cleavage.

A summary of the mechanism for perhydrolysis of **1c** is now possible. Initial attack favors trigonal bipyramid **2f1** by a factor of more than 600:1, and **2f1** rapidly interconverts to **2f2**. However, in contrast to the case of alkaline hydrolysis, P−O bond cleavage from **2f2** cannot compete with either pseudorotation to **2e1** or rearrangement to **5**. In fact, pseudorotation followed by P−S bond cleavage will be about 12 orders of magnitude faster than P−O bond cleavage. With neither a complete pseudorotational potential energy surface nor complete data for the presumably rapid reaction of **5** to **3c**,[29,80] we cannot distinguish between the exit channels from **2f2**. However, we have clearly demonstrated that P−S bond cleavage can be realized from trigonal bipyramid **2f2**, while P−O bond cleavage cannot.

It should be mentioned that in the actual alkaline hydrolysis experiment, **3c** and **4c** are the observed organophosphorus products, but methoxide and methylthiolate are produced due the presence of excess base. In the perhydrolysis experiment, **4c** is the only observed

organophosphorus species but several sulfur moieties are formed.[15,22] Rather than attempt to model the oxidation−reduction chemistry necessary to account for the various products, we have chosen to use as our organophosphorus products **3c** and **4c** for alkaline hydrolysis and **3d** and **4d** for perhydrolysis. This gives methanol and methanethiol as the leaving groups in both cases, allowing a study of trends caused solely by changing the nucleophile. Thus, neither our final products nor ΔH_{rxn} values are directly comparable to those from experiment, but the computed $\Delta\Delta H_{rxn}$ values do reflect the thermodynamic trends appropriately. There are no such concerns regarding the intermediate species, and these should accurately reflect the true chemical processes. Furthermore, the overall enthalpy change is not important to our conclusions since the primary factor determining product ratios is found to be the fate of the trigonal bipyramid with methoxide apical (**2d** or **2f**).

Conclusions

Ab initio molecular orbital and density functional calculations have been carried out on the alkaline hydrolysis of sarin and a VX model compound and the perhydrolysis of the VX model. For the alkaline hydrolysis of sarin, excellent agreement with the experimental enthalpies of activation[11,12] was found at the MP2//mPW1K/MIDI! + ΔG_{solv2} level of theory, which was chosen as the best compromise between accuracy and efficiency. While there are known deficiencies with the solvation calculations in particular, this composite level of theory appears to be appropriate for examining the chemistry of organophosphorus compounds. The computed data offer additional support for the commonly accepted two-step addition−elimination pathway involving a trigonal bipyramidal intermediate, where attack of the nucleophile is the rate-determining step.

For the reactions of VX model **1c**, a number of similarities can be found between the reactions with hydroxide and the reactions with hydroperoxide. The data show that a two-step addition−elimination mechanism is likely with both nucleophiles and it is kinetically favorable for the nucleophile to attack opposite the more apicophilic methoxide ligand. This preference carries through to the trigonal bipyramidal intermediates, where the trigonal bipyramid with methoxide apical (**2d** or **2f**) is thermodynamically more stable than the trigonal bipyramid with methylthiolate apical (**2c** or **2e**). With either nucleophile, it is predicted that **2d/f** is essentially the sole product of nucleophilic attack, based upon kinetic arguments. In both alkaline hydrolysis and perhydrolysis, the fate of trigonal bipyramid **2d/f** determines the product ratio, but the potential energy surfaces of the two reactions contrast dramatically at this point. In alkaline hydrolysis, loss of methoxide from **2d2** competes with pseudorotation of **2d2** to **2e1** and subsequent loss of methylthiolate, resulting in a mixture of P−O and P−S bond cleavage. In perhydrolysis, either pseudorotation of **2f2** to **2e1** followed by P−S bond cleavage or internal rearrangement of **2f2** to **5** is substantially favored over P−O bond cleavage from **2f2**. Regardless of the precise fate of **2f2**, the P−S bond is efficiently cleaved while no P−O bond cleavage is predicted.

While each of the above observations is consistent with the available experimental data,[15,16,26] we must comment further on the role of oxidation. In oxidizing solutions, it has been demonstrated that oxidation at sulfur precedes hydrolysis, and this is an important consideration in the perhydrolysis chemistry.[17] The net effect of such oxidation is likely to make P−S bond cleavage even more facile than in the unoxidized case considered here by weakening the P−S bond,[81] but further work will be necessary to quantify this assumption. Nevertheless, we have shown that nucleophilic attack on *O,S*-dimethyl methylphosphonothiolate gives stable trigonal bipyramidal structures, the fate of which determine the product ratio, and that all salient experimental trends are reproduced by our computations.

Acknowledgment. J.S., J.L.M., R.J.E., and E.V.P. gratefully acknowledge the office of the Vice President of Academic Affairs, Division of Science and Chemistry Alumni Research Fund of Truman State University for their support of this work. C.J.C. thanks the NSF (CHE-0203346) for partial support of this work. Preliminary efforts leading to this work were supported by Army Research Office Grant DAAH04-96-1-0424 (C.J.C. and E.V.P.). Cover artwork design by Winston Vanderhoof of Truman State University Publications.

Supporting Information Available: Cartesian coordinates of all geometries optimized at all levels of theory referenced, along with E(SCF), E(MP2), and ΔG_{solv} energies and number of imaginary vibrational modes. This material is available free of charge via the Internet at http://pubs.acs.org.

JO0502706

(81) Corbett, K. M.; Wright, J. B.; White, W. E. *Proceedings of the November 1998 ERDEC Scientific Conference of Chemical and Biological Defense Research*; Aberdeen Proving Ground, MD, 1999; pp 643−650.